A SPIRAL SHAPED SLOT AS A BROAD-BAND SLOT-TED WAVEGUIDE ANTENNA

Ali Daliri[1, *], Amir Galehdar[1], Wayne S. T. Rowe[1], Kamran Ghorbani[1], Chun H. Wang[2], and Sabu John[2]

[1]School of Electrical and Computer Engineering, RMIT University, Melbourne, VIC 3001, Australia

[2]School of Aerospace, Mechanical and Manufacturing Engineering, RMIT University, Bundoora, VIC 3083, Australia

Abstract—The utility of slotted waveguide antennas would be maximized if the bandwidth of the radiating elements matched that available in the waveguide. This was achieved using a spiral shaped slot cut through the broad-wall of a rectangular waveguide. The predicted total efficiency and peak realized gain were relatively uniform across the entire bandwidth. The current distribution around the slot was predicted to be similar to that around a conventional, center fed, slot spiral antenna, indicating similarity of radiation mechanisms. Finally, the antenna patterns for spiral shaped slots in waveguides manufactured from copper and carbon fibre reinforced polymer (CFRP) were shown to be similar to that predicted.

1. INTRODUCTION

Antennas are critical in many modern vehicles because they transition radiofrequency (RF) waves between internal systems and free space. The traditional approach to install antennas on vehicles is to fasten each as a separate unit to the exterior or under a radome. This (i) degrades vehicle performance (speed, range, endurance and payload) because of redundant weight and volume, and (ii) constrains antenna size and location because of signal masking and RF/physical interference with other systems.

Conformal Load-bearing Antenna Structure (CLAS) overcomes these limitations by integrating antennas into the vehicle structure. CLAS also allows the (i) individual antenna elements to be larger,

thereby allowing operation at different frequencies and thus enhancing sensing capabilities, and (ii) antenna arrays to be longer thereby creating narrower beams that enable precision sensing, secure communications and satellite communications [1]. One type of antennas used for radar and satellite communications in the aerospace and aviation industry is the Slotted Waveguide Antenna (SWA). SWAs date back to World War II and were popular from the 1940s to the 1970s because of their simplicity, high power handling capacity and relatively low profile. A comprehensive review of SWAs is given in [2]. The electrical and mechanical requirements of SWAs for radar applications are summarized in [3].

SWAs may operate in standing or travelling wave mode and the slots used are called resonant or non-resonant slots, respectively. Most SWAs are resonant where an electrical short at the end of the waveguide reflects the incoming RF to create a standing wave within the waveguide. The slots are approximately half a wavelength long and centered under the peaks in the standing wave. These antennas are very narrow-band, with band-widths in the order of 3%. The travelling wave mode enables broad-band behaviour. This mode is created by placing an absorber at the far end of the waveguide, which prevents the formation of a standing wave. In travelling wave antennas the slot sizes and locations are fixed, which results in the beam direction varying with frequency, a phenomenon called frequency scanning [4].

SWAs are traditionally manufactured from metals such as copper, brass or aluminium. For weight critical applications such as satellite antennas, SWAs have been manufactured from CFRP. In 1980, a narrowband slotted waveguide array antenna was developed by the European Space Agency for a satellite based Synthetic Aperture Radar (SAR) [5].

One form of CLAS, known as Slotted Waveguide Antenna Stiffened Structure (SWASS), integrates Slotted Waveguide Antennas (SWAs) into the load-bearing vehicle structure (see Figure 1). In SWASS the blade stiffeners in sandwich panels or top-hat stiffeners on skins serve the dual purpose of providing both structural stiffening and serving as RF waveguides. SWAs are produced by cutting slots through the outer skin and into the waveguides. Finally, these slots are filled with a RF transparent dielectric to restore the outer mould line.

The SWASS concept was introduced in [1] and methods of manufacture are described in [6, 7]. It was shown that SWASS antennas could be manufactured from aerospace grade Carbon Fibre Reinforced Polymer (CFRP). The characteristics of SWAs made from CFRP operating at X-band were compared with those manufactured from
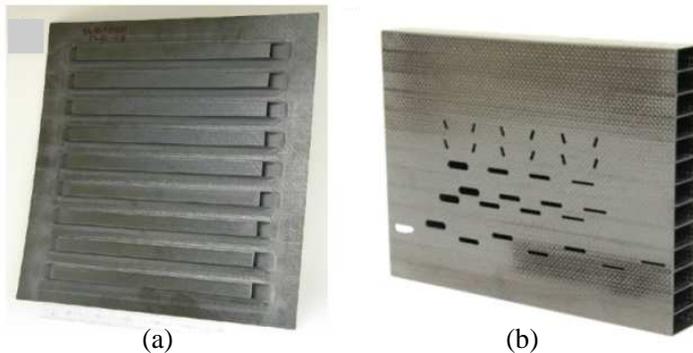
Figure 1. SWASS panel concept (b) developed by the integration of slotted waveguide antennas into the hat stiffener aircraft panel (a) [9].

aluminium and copper in [8, 9]. The antenna patterns were similar in shape to those from metallic SWAs but gain was lower because of the ohmic loss in the composite.

The utility of a SWASS antenna would be maximised if the slots operate across the entire bandwidth that is available in the waveguide. This is in the order of 40% for rigid rectangular waveguides. For example WR-90 waveguides operate, in the fundamental Transverse Electric, TE_{10}, mode from 8.2–12.4 GHz. Spiral antennas are well known for their wideband characteristics and have been used since the 1950s [10–12]. They can easily cover a 40% bandwidth and, if they could be incorporated into SWASS, would allow the full bandwidth available in the waveguide to be exploited. However, traditional spiral antennas cannot be used for SWASS application because they require a cavity behind the radiating element and they need to be mounted on the surface of the airplane. They also require a balanced feed at the center of each element of an array which makes their application in SWASS impossible.

One way to integrate the spiral antenna into the SWASS concept is to cut spiral slots on the broad wall of rectangular waveguides where spiral slots are part of a SWA array. In this case, the spiral slots act similar to rectangular slots cut on the broad wall of the waveguide and they need to be studied as elements of a SWA array rather than standalone traditional spiral antennas. Spiral configuration of rectangular slots [13, 14] cannot be used for SWASS where hat stiffeners in the airplane skin operate as rectangular waveguides not radial waveguides. A continuous spiral slot has not yet been used as an element of rectangular SWA arrays.

Different slot shapes have been proposed recently for SWA array application. For example, an inclined semi-circular slot cut in the narrow wall of a rectangular waveguide was proposed for X-band arrays [15]; however, this antenna is narrowband. In [16] a travelling-wave sinusoidal SWA was applied to the short-wall of a waveguide and proposed for operation in the Ka-band. However, a slot shape that can be cut on the broad wall of a rectangular waveguide and be integrated into hat stiffener panels and provide full X-band coverage has not yet been reported in the literature.

In this paper, we show that a spiral slot cut into the broad wall of a WR-90 rectangular waveguide acts as a broad-band travelling wave radiator. This slot shape covers almost the entire X-band and can be easily integrated into SWASS panels as an element of an array. The novel integration of spiral slots in rectangular waveguides is a new solution for the limited bandwidth of SWASS and as far as the authors are aware, this has hitherto not been reported in the publicly available literature. The surface current distribution of this slot at three different frequencies was simulated and compared with that in a conventional slot spiral antenna to explain its broad-band characteristics. The total electrical efficiency and peak realized gain of this slot were compared with those of a rectangular slot which is the current slot shape used in SWASS. The gain patterns from an optimised spiral shape slot were simulated and confirmed by measurement.

2. SPIRAL SHAPED SLOTTED WAVEGUIDE ANTENNA

2.1. Design

The spiral shaped slot was designed to be incorporated into the broad-wall of WR-90 rigid rectangular waveguides and operate across the X-band (8–12 GHz). The internal cross-sectional dimensions of WR-90 waveguides are 22.86 mm × 10.16 mm, which is of the same order as hat stiffeners on skins or face-sheet separation in CFRP aircraft structures [1]. Previous SWASS development has been conducted on CFRP waveguides with the same internal cross-section [7–9].

The slot shape selected was a self-complementary, two-slot, equiangular spiral. The ends of the spiral slots were terminated with a semi-circle in order to minimise the stress concentration [17]. Slots were simulated using the HFSS^{TM} (version 14.0) software. A parametric study was performed to determine the slot geometry that would radiate over the entire X-band. The optimized design parameters are shown in Table 1.

Table 1. Design parameters and optimized values.

Parameter	Description	Optimized value
Slot width angle	Width of spiral slots	$\pi/2$
Growth rate	Spiral tightness	0.178
Number of turns	Number of spiral turns	1 turn
Inner radius	Controls max. operating frequency	3.67 mm
Outer radius	Controls min. operating frequency	11.25 mm

A traditional longitudinal, broad-wall, rectangular slot was used for comparison. This slot was designed to resonate at 10 GHz but it would be operated in travelling wave mode for this work. It was 15.00 mm long by 2.00 mm wide. The slot ends were rounded with 1.00 mm radius and slot offset from the broad wall's centerline was 6.50 mm. The waveguide wall thickness was 1.27 mm for both slot antennas, which matches that of a standard metal WR-90 waveguide.

2.2. Surface Current Distribution

Slot antennas radiate as a result of time varying currents around the periphery of the slot. The currents around slots in waveguide walls will be induced by the RF waves propagating within the waveguide. These waves sweep across the slot, radial at the leading and trailing edges and tangential at the lateral tips. This contrasts with conventional, center-fed, slot spirals where the RF wave is launched at the center and it sweeps outward along the spiral.

In order to explain the broad-band performance of the proposed spiral shaped slot the surface current distribution needs to be studied. For such a study, the surface current distribution of a conventional center-fed spiral slot antenna was also simulated and presented here. A schematic showing the two feed configurations is shown in Figure 2. First, the spiral slot cut into the broad wall of a waveguide was simulated by enabling Wave Ports 1 and 2 (operating at the TE_{10} mode) and disabling the Lumped Port. This feeding mechanism was used for the Figures 4 to 19. Then a more conventional spiral slot feeding was simulated by enabling the Lumped Port (with the dominant mode of operation) and the two Wave Ports. Both simulations were conducted using the same model geometry (a spiral shaped slot in a waveguide) in order to allow direct comparison of the
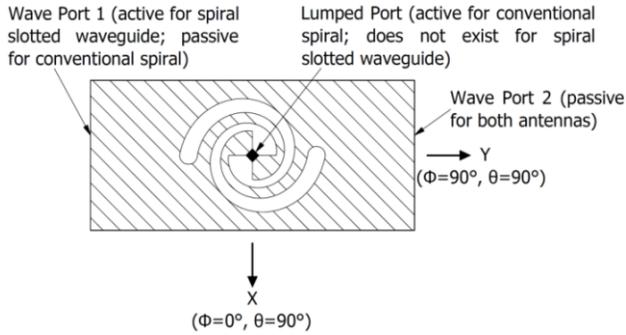
Figure 2. A schematic of the two feeding configurations used to predict surface current distribution around the spiral shaped slot on the broad wall of a rectangular waveguide.
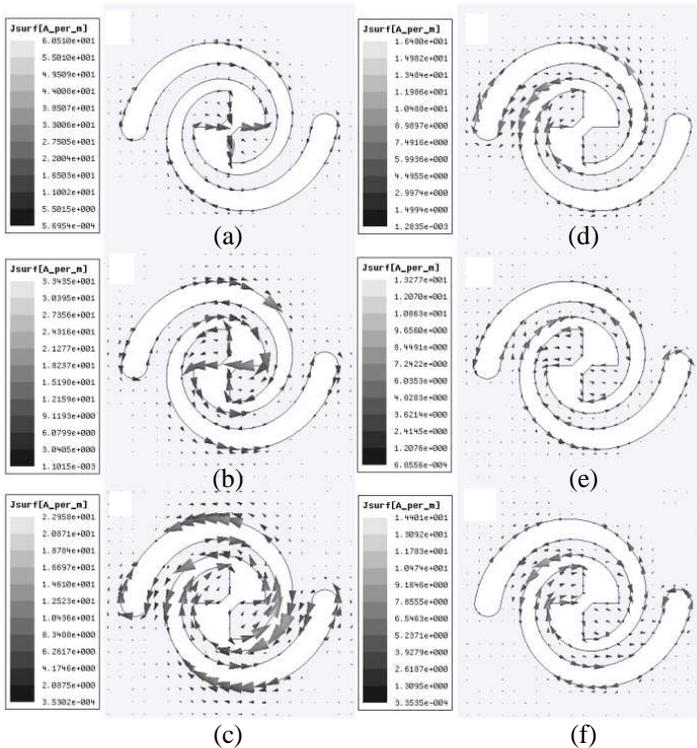
Figure 3. Surface current distribution for conventional center-fed spiral at (a) 9 GHz, (b) 10 GHz, and (c) 11 GHz, and waveguide-fed spiral shaped slot at (d) 9 GHz, (e) 10 GHz, and (f) 11 GHz.

results.

The simulated surface current distribution for the two different methods of feeding at 9, 10 and 11 GHz are shown in Figure 3. It is apparent that, regardless of the feed, the surface currents were sinusoidal along the length of the spiral arms and in opposite directions on opposing slot faces. In addition the locations of peak current rotated clockwise along the slot arms as frequency increased. The relative position and magnitude of these peaks were different for the two types of feed. At 9 GHz the current pattern on the upper slot arms were very similar for both of the feeding methods (Figures 3(a) and (d)); whilst at 11 GHz the pattern on the lower arms was almost identical (Figures 3(c) and (f)). This similarity in the pattern is true for both arms at 10 GHz (Figures 3(b) and (e)).

The similarity in the surface current distribution of the conventional fed spiral and the spiral slot on the waveguide in at least one arm explains why the later shows broad-band characteristics. In addition, the phase different between the second arms of the spiral slot and the conventional fed spiral explains why it has elliptical polarisation rather than circular polarisation expected from the spiral shape.

2.3. Efficiency and Realized Gain

It is intended that the spiral shaped slot antenna developed in this work would replace rectangular resonant slots. The antenna performance of these two antenna types were therefore predicted and compared. The predicted total efficiency (radiated power divided by the input power) is shown in Figure 4. Here, the total efficiency is used instead of the radiation efficiency to account for the power transmitted to the second port of the waveguide. This shows what percentage of the power incident to the first port of the waveguide is radiated by the spiral shaped slot and what percentage of the power is left for other elements of the SWA array. The behavior of the rectangular slot is characteristic of resonant antennas. Efficiency is high at resonance and low elsewhere. In contrast the total efficiency of the spiral shaped slot was moderate, with variation of only 8%, across the X-band.

This is consistent with the predicted peak realized gain shown in Figure 5. The realized gain was shown instead of gain in order to account for the power transmitted to the second port of the waveguide. The bandwidth of the conventional rectangular slot based on its realized gain and total efficiency is narrow whilst for the spiral shaped slot the peak realized gain is relatively uniform across the entire X-band.
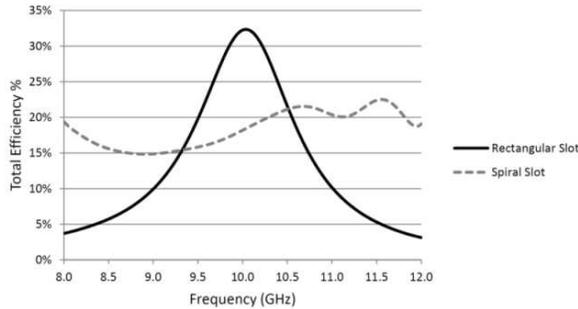
Figure 4. The predicted total efficiency for a rectangular slot resonating at 10 GHz and the spiral slot on the waveguide broad-wall.
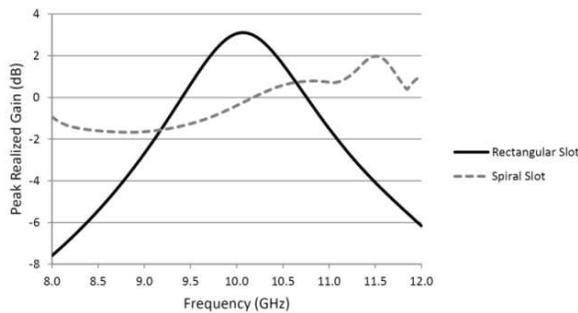
Figure 5. The predicted peak realized gain for a rectangular slot resonating at 10 GHz and the spiral slot on the waveguide broad-wall.

3. EXPERIMENTAL VALIDATION

Waveguides were manufactured, spiral antennas cut and RF performance measured in order to validate the simulations described in the previous sections. Figure 6 shows spiral shaped slot radiators machined into waveguides manufactured from copper and CFRP. The CFRP was aerospace grade Cytec IM7/977-3 unidirectional prepreg tape with a [0 90]s ply stacking sequence. The autoclave cured waveguides had a wall thickness of 0.5 mm.

The simulated and measured scattering parameters $|S_{11}|$ and $|S_{21}|$) are shown in Figure 7. $|S_{11}|$ was below -10 dB from 8.5–12.0 GHz indicating coverage of almost the entire X-band. There was excellent agreement between the simulated and measured S-parameters for the copper waveguide. The difference in S-parameters between the CFRP

Figure 6. Spiral SWA manufactured from copper and brass flanges (upper image), and CFRP and aluminium flanges (lower image).
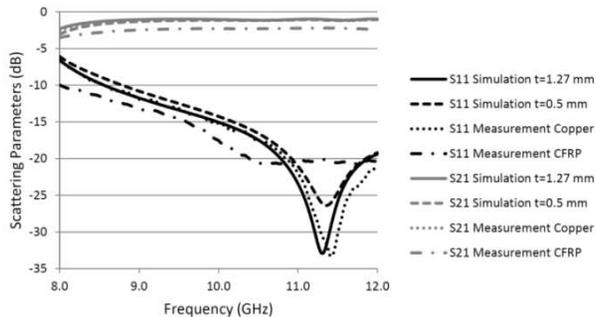
Figure 7. The simulated and measured S-parameters for the spiral shaped SWA ('t' refers to the simulated waveguide wall thickness).

and copper waveguides are due to the insertion loss in the CFRP which is well described in [8, 18–20]. This resulted in the $|S_{21}|$ for the spiral shaped SWA in CFRP to be approximately 1 dB lower than that in the metallic waveguide throughout the band.

The radiation pattern of the manufactured antennas was measured in an anechoic chamber. One end of the waveguide was connected to a SMA-to-waveguide adapter (HP® X281A$^{\text{TM}}$) and the far-end of the waveguide connected to a waveguide termination (NSN: 5985-99-527-1086). This produced a travelling wave in the waveguide. Both the adapter and the termination were covered with absorber material to minimise ripples in the radiation pattern arising from inadvertent reflections from these items.

The simulated and measured realized gain patterns on the E-plane ($\Phi = 90°$) and H-plane ($\Phi = 0°$), for H-H and V-V polarisations, at 9, 10 and 11 GHz, are shown in Figures 8 to 19. The patterns that are shown for these three frequencies show the frequency scanning, although maximum gain is generally close to the broadside direction ($\Phi = \theta = 0°$). For horizontal polarisation the main beam scanned with frequency from approximately $-30°$ at 9 GHz (Figures 8 and 10) to approximately $0°$ at 11 GHz (Figures 16 and 18). For vertical
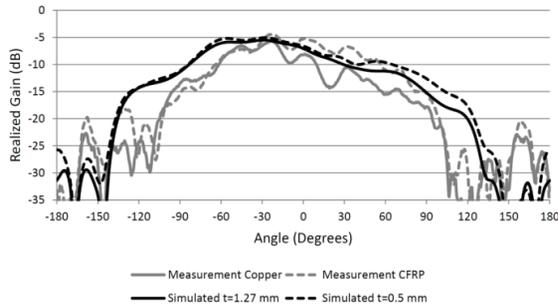
Figure 8. Realized gain (theta) at $9\,\text{GHz}$ ($\Phi = 90°$). 't' refers to the simulated waveguide wall thickness.
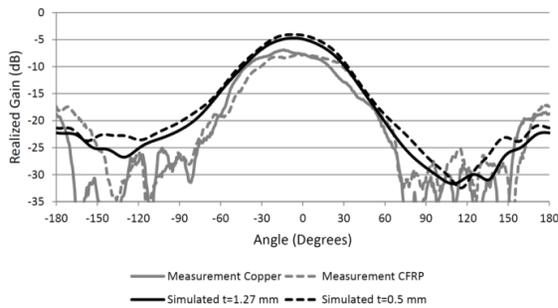
Figure 9. Realized gain (phi) at $9\,\text{GHz}$ ($\Phi = 90°$). 't' refers to the simulated waveguide wall thickness.

polarisation the main beam was approximately at $0°$ for all frequencies except at $11\,\text{GHz}$ (Figure 17). Also, from Figures 8 to 19 it is apparent that the spiral slot shows elliptical polarisation. The axial ratio of the antenna is about $10\,\text{dB}$ across the entire frequency band which is caused by the phase difference in the spiral arms. This behaviour makes the antenna suitable for applications such as meteorological radar [21, 22], or applications where polarization purity is not a concern.

The measured results were generally in good agreement with simulations. Differences between measured and simulated realized gain for the copper waveguides are attributed to the approximately (i) $0.5\,\text{dB}$ accuracy of measurement in the anechoic chamber, (ii) $0.5\,\text{dB}$ loss in the SMA-to-waveguide adapter, (iii) non-ideal travelling wave condition resulted from the non-ideal waveguide termination, and (iv) slot machining tolerances. For the CFRP spiral shaped SWA, the measured pattern was also influenced by the loss in the waveguide walls and anisotropic properties of the CFRP.
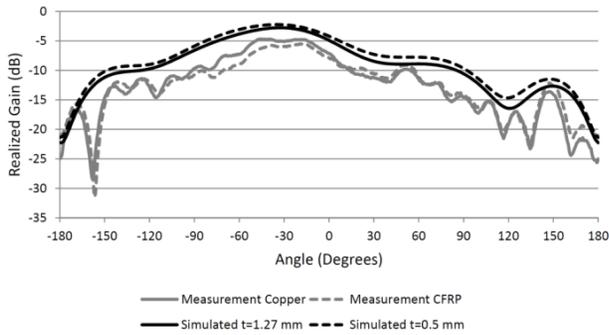
Figure 10. Realized gain (theta) at $9\,\text{GHz}$ ($\Phi = 0°$). 't' refers to the simulated waveguide wall thickness.
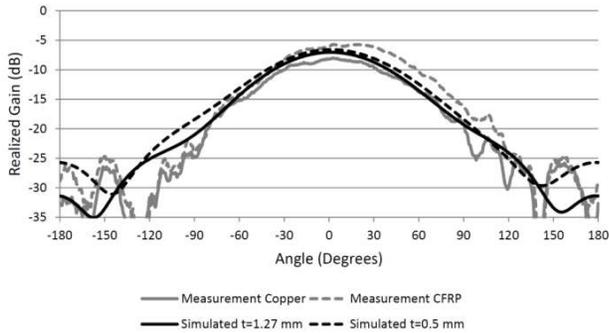
Figure 11. Realized gain (phi) at $9\,\text{GHz}$ ($\Phi = 0°$). 't' refers to the simulated waveguide wall thickness.
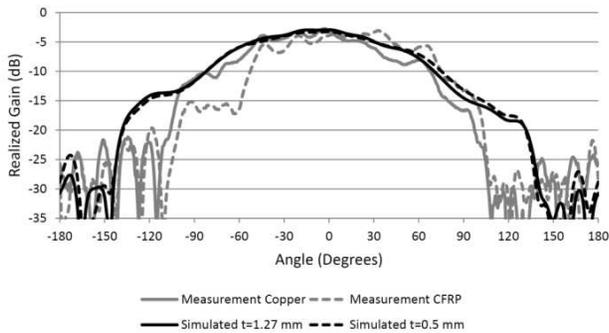
Figure 12. Realized gain (theta) at $10\,\text{GHz}$ ($\Phi = 90°$). 't' refers to the simulated waveguide wall thickness.
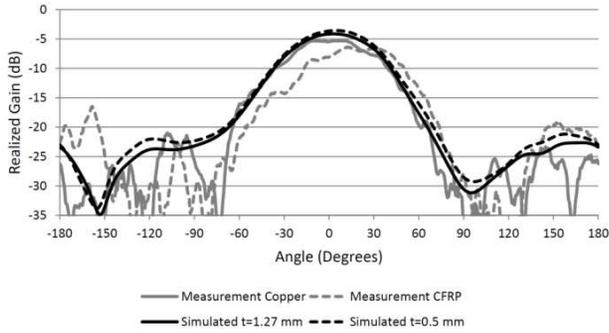
Figure 13. Realized gain (phi) at 10 GHz ($\Phi = 90°$). 't' refers to the simulated waveguide wall thickness.
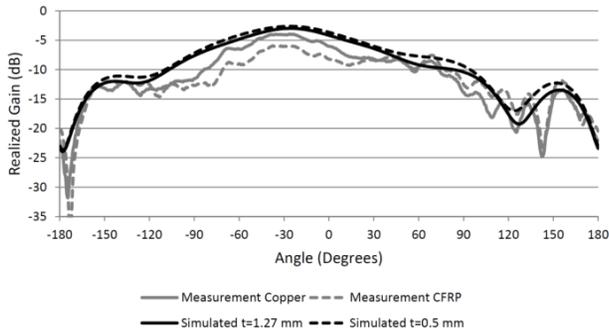
Figure 14. Realized gain (theta) at 10 GHz ($\Phi = 0°$). 't' refers to the simulated waveguide wall thickness.
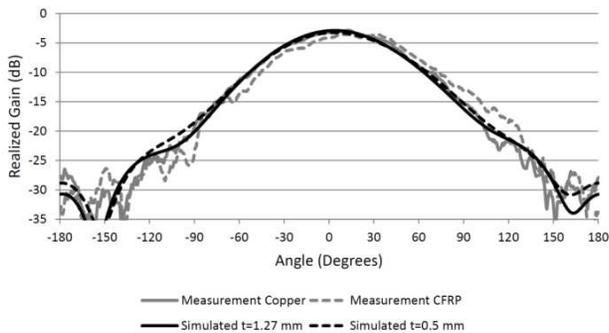
Figure 15. Realized gain (phi) at 10 GHz ($\Phi = 0°$). 't' refers to the simulated waveguide wall thickness.
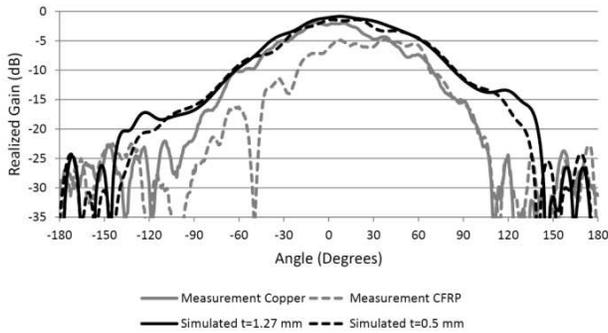
Figure 16. Realized gain (theta) at 11 GHz ($\Phi = 90°$). 't' refers to the simulated waveguide wall thickness.
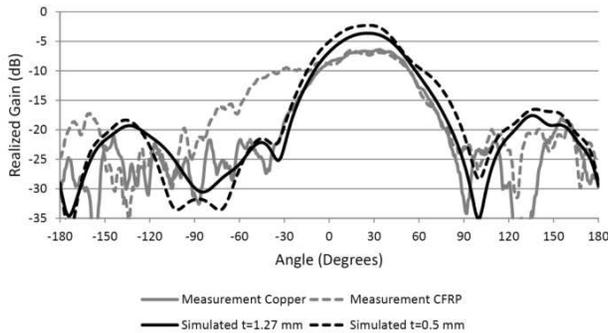
Figure 17. Realized gain (phi) at 11 GHz ($\Phi = 90°$). 't' refers to the simulated waveguide wall thickness.
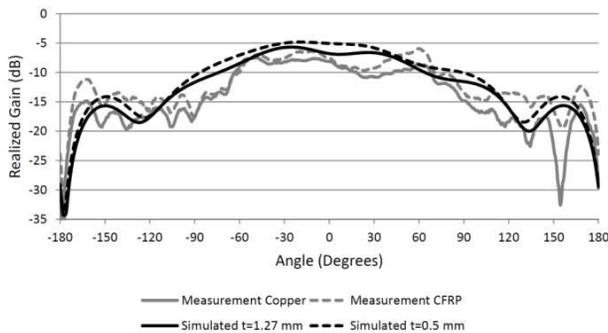
Figure 18. Realized gain (theta) at 11 GHz ($\Phi = 0°$). 't' refers to the simulated waveguide wall thickness.
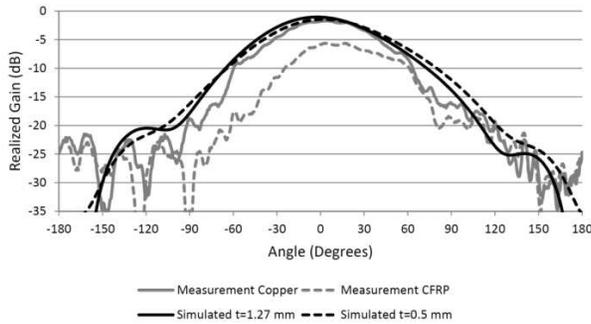
Figure 19. Realized gain (phi) at $11\,\mathrm{GHz}$ ($\Phi = 0°$). 't' refers to the simulated waveguide wall thickness.

4. CONCLUSION

Spiral shaped slots cut through the broad-wall of a WR-90 rectangular waveguide can be designed to radiate over almost the entire X-band. The surface currents around these slots are predicted to be similar to those around conventional, center-fed, spiral slot antennas. The total efficiency and peak realized gain of the spiral shaped slot are predicted to be approximately uniform across the band, in contrast to the resonance that is characteristic of conventional rectangular slots. The total efficiency of the spiral shaped slot was about 20%, with variation of only 8%, across the X-band. The antenna realized gain has $\pm 2\,\mathrm{dB}$ variation across the X-band showing a superior flat gain response compared to resonant slots. This efficiency and gain performance is suitable for SWA array applications.

The scattering parameters and antenna patterns of antennas manufactured from copper and aerospace grade carbon fibre reinforced polymer were measured and shown to match the predictions. The $-10\,\mathrm{dB}$ impedance bandwidth of this antenna is 35%, indicating coverage of almost the entire X-band range. The proposed spiral shaped slot possesses elliptical polarisation. This broad-band element is expected to enable broad-band conformal load-bearing antenna structures such as Slotted Waveguide Antenna Stiffened Structure.

ACKNOWLEDGMENT

REFERENCES

1. Callus, P. J., *Novel Concepts for Conformal Load-bearing Antenna Structure*, Tech. Rep. DSTO-TR-2096, DSTO Air Vehicles Div., Melbourne, VIC, Feb. 2008, http://hdl.handle.net/1947/9300.

2. Rengarajan, S. R., L. G. Josefsson, and R. S. Elliott, "Waveguide-fed slot antennas and arrays: A review," *Electromagnetics*, Vol. 19, No. 1, 3–22, 1999.

3. Forrester, R. W. and D. R. Morgan, "The mechanical design and manufacture of a high performance airborne radar antenna," *Proc. IEE Colloquium on Mechanical Aspects of Antenna Design*, 11/1–11/5, London, Apr. 1989.

4. Solbach, K., "Below-resonant-length slot radiators for traveling-wave-array antennas," *IEEE Antennas and Propagation Mag.*, Vol. 38, No. 1, 7–14, 1996.

5. Wagner, R. and H. M. Braun, "A slotted waveguide array antenna from carbon fibre reinforced plastics for the European space SAR," *Acta Astronautica*, Vol. 8, No. 3, 273–282, 1981.

6. Noble, W. J. and J. W. Small, *Lightweight Composite Slotted-waveguide Antenna and Method of Manufacture*, US Patent 4255752, Mar. 10, 1981.

7. Callus, P. J. and K. J. Nicholson, *Standard Operating Procedure — Manufacture of Carbon Fibre Reinforced Plastic Waveguides and Slotted Waveguide Antennas*, Tech. Note DSTO-TN-0937, Version 1.0, DSTO Air Vehicles Div., Melbourne, VIC, Jun. 2011, http://hdl.handle.net/1947/10149.

8. Gray, D., K. J. Nicholson, K. Ghorbani, and P. J. Callus, "Carbon fibre reinforced plastic slotted waveguide antenna," *Proc. Asia-Pacific Microwave Conf.*, 307–310, Yokohama, Dec. 2010.

9. Nicholson, K. J. and P. J. Callus, *Antenna Patterns from Single Slots in Carbon Fibre Reinforced Plastic Waveguides*, Tech. Rep. DSTO-TR-2389, DSTO Air Vehicles Div., Melbourne, VIC, Feb. 2010, http://hdl.handle.net/1947/10048.

10. Dyson, J., "The equiangular spiral antenna," *IRE Trans. Antennas and Propagation*, Vol. 7, No. 2, 181–187, 1959.

11. Turner, E. M., *Spiral Slot Antenna*, US Patent 2863145, Dec. 2, 1958.

12. Amin, Y., Q. Chen, L. R. Zheng, and H. Tenhunen, "Design and fabrication of wideband archimedean spiral antenna based ultra-low cost "green" modules for RFID sensing and wireless applications," *Progress In Electromagnetics Research*, Vol. 130, 241–256, 2012.

13. Ando, M., K. Sakurai, N. Goto, K. Arimura, and Y. Ito, "A radial line slot antenna for 12 GHz satellite TV reception," *IEEE Trans. Antennas and Propagation*, Vol. 33, No. 12, 1347–1353, 1985.

14. Takahashi, M., J. I. Takada, M. Ando, and N. Goto, "A slot design for uniform aperture field distribution in single-layered radial line slot antennas," *IEEE Trans. Antennas and Propagation*, Vol. 39, No. 7, 954–959, 1991.

15. Ghafoorzadeh, A. and K. Forooraghi, "Analysis of an inclined semi-circular slot in the narrow wall of a rectangular waveguide," *Progress In Electromagnetics Research*, Vol. 90, 323–339, 2009.

16. Salman, A. O., "Millimeter-wave sinusoidal slotted waveguide antenna," *Int. Kharkov Symp. Physics and Engineering of Microwaves, Millimeter and Submillimeter Waves (MSMW)*, 1–4, Kharkiv, Jun. 2010.

17. Daliri, A., A. Galehdar, C. H. Wang, W. S. T. Rowe, S. John, K. Ghorbani, and P. J. Callus, "FEA evaluation of mechanical and electromagnetic performance of slot log-spiral CLAS," *Proc. the ASME Conf. Smart Materials, Adaptive Structures and Intelligent Systems (SMASIS)*, Phoenix, Sep. 2011.

18. Galehdar, A., W. S. T. Rowe, K. Ghorbani, P. J. Callus, S. John, and C. H. Wang, "The effect of ply orientation on the performance of antennas in or on carbon fiber composites," *Progress In Electromagnetics Research*, Vol. 116, 123–136, 2011.

19. Bojovschi, A., K. J. Nicholson, A. Galehdar, P. J. Callus, and K. Ghorbani, "The role of fibre orientation on the electromagnetic performance of waveguides manufactured from carbon fibre reinforced plastic," *Progress In Electromagnetics Research B*, Vol. 39, 267–280, 2012.

20. De Paulis, F., M. H. Nisanci, M. Y. Koledintseva, J. L. Drewniak, and A. Orlandi, "Homogenized permittivity of composites with aligned cylindrical inclusions for causal electromagnetic simulations," *Progress In Electromagnetics Research B*, Vol. 37, 205–235, 2012.

21. Matrosov, S. Y., "Prospects for the measurement of ice cloud particle shape and orientation with elliptically polarized radar signals," *Radio Science*, Vol. 26, No. 4, 847–856, 1991.

22. Krofli, R. A. and R. D. Kelly, "Meteorological research applications of mm-wave radar," *Meteorology and Atmospheric Physics*, Vol. 59, 105–121, 1996.